



An optoacoustic black carbon sensor for ship emission monitoring

Linda Haedrich, Nikolaos Kousias, Ioannis Raptis, Delin Li, Uli Stahl, Leonidas Ntziachristos & Vasilis Ntziachristos

To cite this article: Linda Haedrich, Nikolaos Kousias, Ioannis Raptis, Delin Li, Uli Stahl, Leonidas Ntziachristos & Vasilis Ntziachristos (22 Apr 2025): An optoacoustic black carbon sensor for ship emission monitoring, Aerosol Science and Technology, DOI: [10.1080/02786826.2025.2490642](https://doi.org/10.1080/02786826.2025.2490642)

To link to this article: <https://doi.org/10.1080/02786826.2025.2490642>



© 2025 The Author(s). Published with license by Taylor & Francis Group, LLC.



[View supplementary material](#)



Published online: 22 Apr 2025.



[Submit your article to this journal](#)



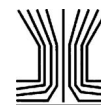
Article views: 201



[View related articles](#)



[View Crossmark data](#)



An optoacoustic black carbon sensor for ship emission monitoring

Linda Haedrich^{a,b} , Nikolaos Kousias^c, Ioannis Raptis^c, Delin Li^{a,b}, Uli Stahl^{a,b}, Leonidas Ntziachristos^c , and Vasilis Ntziachristos^{a,b,d}

^aChair of Biological Imaging, Central Institute for Translational Cancer Research (TranslaTUM), School of Medicine and Health & School of Computation, Information and Technology, Technical University of Munich, Munich, Germany; ^bInstitute of Biological and Medical Imaging, Bioengineering Center, Helmholtz Zentrum München, Neuherberg, Germany; ^cMechanical Engineering Department, Aristotle University of Thessaloniki, Thessaloniki, GR, Greece; ^dMunich Institute of Biomedical Engineering (MIBE), Technical University of Munich, Garching b. München, Germany

ABSTRACT

Black carbon (BC) emitted from ship exhaust has negative impacts on both human health and the climate. Monitoring BC emissions and, potentially, introducing a regulatory framework, will depend on the availability of reliable techniques for the measurement of its emission. Current sensors enabling continuous monitoring are too expensive and require frequent maintenance. We have recently developed a low-cost optoacoustic (OptA) BC sensor, which spatially separates OptA detection from OptA excitation, and demonstrated its performance in the laboratory. The unique chamber-based design of the sensor allows for the spatial separation of its delicate quartz tuning fork (QTF) detector from BC particles, while reaching high sensitivity without the need for filters. In this work, we examine for the first time the sensor operation in a real environment, by implementing it on-board a roll-on-roll-off (RoRo) ferry transporting cargo and passengers (RoPax). We present longitudinal measurements of BC concentrations within the ship's exhaust. We observe a strong linear correlation ($R^2 = 0.9$) between our OptA sensor to an aerosol absorption photometer, used for comparison. BC concentrations of the ships exhaust were measured directly from the funnel and BC emission factors were estimated based on simultaneously measured CO₂ content of the exhaust and the carbon content of the fuel. BC concentrations were found to vary depending on the fuel used, namely, marine gas oil (MGO) and methanol. For the latter significantly reduced BC concentrations were observed. We finally discuss the implications of the technology for low-cost and low-maintenance sensors for on-board BC monitoring and beyond.

ARTICLE HISTORY

Received 28 October 2024

Accepted 24 March 2025

EDITOR

Jingkun Jiang

CONTACT Vasilis Ntziachristos bioimaging.translatum@tum.de Chair of Biological Imaging, Central Institute for Translational Cancer Research (TranslaTUM), School of Medicine and Health & School of Computation, Information and Technology, Technical University of Munich, Munich, Germany.

Supplemental data for this article can be accessed online at <https://doi.org/10.1080/02786826.2025.2490642>.

© 2025 The Author(s). Published with license by Taylor & Francis Group, LLC.

This is an Open Access article distributed under the terms of the Creative Commons Attribution License (<http://creativecommons.org/licenses/by/4.0/>), which permits unrestricted use, distribution, and reproduction in any medium, provided the original work is properly cited. The terms on which this article has been published allow the posting of the Accepted Manuscript in a repository by the author(s) or with their consent.

GRAPHICAL ABSTRACT

An Optoacoustic Black Carbon Sensor for Ship Emission Monitoring

Original Article



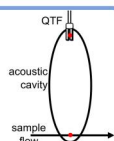
Black carbon (BC) from ship emissions contribute to increased melting of snow and ice in the Arctic and poor air quality in harbor cities.

To enforce regulations, monitoring of BC emissions is required. However, current BC sensors are expensive and/ or require frequent maintenance.

We present the first integration of a novel optoacoustic (OptA) sensor on-board a RoPAX ferry.

The illumination-detection separating sensor (IDSS):

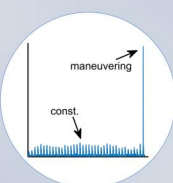
- uses a low-cost quartz tuning fork (QTF)
- has an ellipsoidal acoustic cavity, which allows for spatial separation of QTF and sample flow to prevent contamination.



Observations during the ship-board campaign



Strong linear correlation between the IDSS and an aerosol absorption photometer



Constant BC concentrations for constant ship load
Larger BC concentrations with fast dynamics during maneuvering in the harbor



Significantly reduced BC concentrations for methanol in comparison to marine gas oil (MGO)

An Optoacoustic Black Carbon Sensor for Ship Emission Monitoring
Haedrich et al. (2025) Aerosol Science and Technology

1. Introduction

Black carbon (BC) is generated in incomplete combustion processes, which originate mainly from anthropogenic activities (Bond et al. 2013; Timonen et al. 2019). BC is considered to significantly contribute to climate change (Bond et al. 2013; Harmsen et al. 2020, Pörtner et al. 2022). It strongly absorbs light in the visible and near-infrared spectrum and therefore contributes directly to the solar heating of the atmosphere (Kang et al. 2020). Although marine shipping only contributes around 1.5% of total global BC emissions (Hoesly et al. 2024), these emissions have outsized impacts in several areas. One specific area of concern is the emission of BC in remote regions, such as near or in the Arctic (Bond et al. 2013), which accelerates the melting of ice and snow. The retreating sea ice enables the opening of new shipping routes (Ng et al. 2018) and causes more Arctic pollution, resulting in a self-accelerating vicious cycle. Another problem is posed by overly high BC emissions in port cities, which account for up to 16% and 26% of total particulate matter (PM) emissions in

European and Asian cities, respectively (Sorte et al. 2020). BC exposure is linked to several adverse health effects, such as increased risks of cardiovascular and respiratory diseases (Janssen et al. 2011), adverse birth outcomes, and neurological disorders such as Alzheimer's disease and stroke (Grahame, Klemm, and Schlesinger 2014).

Thus, BC emissions from shipping must be monitored and controlled in order to reduce their negative impacts, especially in remote regions and harbor areas. Currently, the International Maritime Organization (IMO) is working toward the establishment of BC monitoring protocols for ships, which will enable the enforcement of emission-regulating legislation (International Maritime Organization (IMO)) 2011, 2015, 2018). The IMO has suggested three candidate technologies for BC monitoring: filter smoke number (FSN) method, laser-induced incandescence (LII) technique and optoacoustic spectroscopy (OptAS), also often referred to as photoacoustic spectroscopy (PAS) (International Maritime Organization (IMO)) 2018). However, widespread uptake of

automated monitoring will be challenging with the current sensors on the market, which are either expensive or require frequent human intervention, such as the smoke number measurement.

Smoke meters quantify FSNs by measuring changes in the reflectance of a filter paper, i.e., its blackening after exposure to BC. Aethalometers or aerosol absorption photometers use a similar technology, which relies on filter-based absorption to detect BC. Filter-based technologies can be biased by the condensation of sulfur oxides (SO_x) and water onto the filter paper (Lappi and Ristimäki 2019). Furthermore, scattering artifacts and filter-loading effects can also affect measurements (Davies et al. 2019), resulting in inaccurate readings despite elaborate baseline corrections (Coen et al. 2010; Drinovec et al. 2015). Finally, these devices cannot carry out real-time measurements, as there is a time lag between BC emission and its accumulation on the filter paper for measurement (Aakko-Saksa et al. 2021). Some aethalometers have been implemented in shipboard measurement campaigns (Aakko-Saksa et al. 2021, Johnson et al. 2017; Timonen et al. 2017). However, these sensors have been developed to measure BC in low-concentration environments (e.g., urban BC levels). As such, filter-based devices are not suited for measuring high BC concentrations on ships because they then require frequent, even daily, changes of the filter papers. This daily maintenance is obviously cumbersome for vessel crews and it increases the cost of measurement.

LII uses high-powered lasers to heat aerosols to temperatures up to 4000 K in order to measure the quasi-black body radiation of the particles (Michelsen et al. 2015). Such systems are developed for research and science purposes but are costly for on-board systems due to the powerful laser required.

Finally, OptAS is a technique that generates acoustic signals by exciting BC with light of varying intensity, i.e., by modulating the light intensity or using light pulses. The signals are recorded by a transducer and are generally proportional to the BC mass concentration (Ma 2018).

Commercially available OptAS instruments for BC monitoring include the AVL Micro Soot Sensor (MSS, AVL, Graz, Austria) and the Photoacoustic Extinctionmeter (PAX, droplet measurement technologies, CO, USA). These instruments are rather high cost, which limits their appeal for widespread implementation to monitor BC on ships. Another OptAS technique, quartz enhanced photoacoustic spectroscopy (QEPAS), uses a quartz tuning fork (QTF), i.e., a piezoelectric resonator as an ultrasound transducer

(Kosterev et al. 2002). Due to the low cost of the QTF and its high sensitivity, which allows the use of inexpensive light sources, QEPAS devices have the potential to operate economically. However, available QEPAS systems are used for gas sensing (Ma 2018; Patimisco et al. 2014) as they are not well suited for aerosol measurement. In particular, the direct exposure of the sensitive QTF to the sample flow very likely leads to particle deposition on the QTF possibly resulting in a loss in sensitivity.

Regular monitoring of BC aboard vessels without human intervention is therefore in need of new sensors and devices. However, the demonstration of new monitoring systems in the field is lacking. We have previously developed an illumination-detection separating sensor (IDSS) (Stylogiannis et al. 2021), based on illumination, using pulse trains and a low-cost QTF for OptA detection, embodied within an ellipsoid chamber. The chamber places the QTF in a position that is not within the sample flow, i.e., it spatially separates the excitation of ultrasound waves from their detection. The design was chosen to mitigate spreading losses, which would normally arise when separating the point of sound detection from generation as the intensity of spherical waves decreases proportionally to the distance from the source. The IDSS exploits the simple geometrical properties of an ellipsoid, which always has two focal points (Capderou 2014). The point of acoustic signal generation, where the laser excites the sample, is placed in one of the focal points and the QTF is placed in the other. Due to this geometry, the sound waves propagating inside the ellipsoidal cavity are focused onto the QTF mitigating spreading losses. The dimensions are chosen such that the sound waves traveling from focal point to focal point interfere constructively at the location of the transducer. However, while we have demonstrated the advantages of the sensor with laboratory measurements (Stylogiannis et al. 2021), this novel design has not been so far demonstrated in real environments. Therefore, in this study, we examined for the first time the sensor operation on-board a Seapacer-class roll-on-roll-off ferry, the Stena Germanica, which transports both cargo and passengers (RoPax). The sensor was used for longitudinal measurements of 9.5 h monitoring BC emission of the ship's main engine 2 (ME2). The IDSS demonstrated minimal change in the transducer's performance during the measurement indicating the spatial separation of illumination and detection prevented deposition of BC particles onto the sensitive transducer. We compared the sensor operation to an aerosol absorption

photometer (ObservAir), i.e., a filter-based instrument. We report a linear relationship of $R^2 = 0.9$ between the two instruments. Furthermore, we were able to compare the BC emissions of ME2 operating on marine gas oil (MGO) to the emissions of a renewable fuel, methanol. We observe a significant reduction in BC concentration under the engine's operation with methanol. We discuss how the IDSS could provide a cheap and responsive device suitable for longitudinal measurements in real-world applications.

2. Materials and methods

2.1. Design of the OptA sensor prototype

The development, construction, and design of the OptA sensor prototype was described previously (Ntziachristos et al. 2021; Stylogiannis et al. 2021). In brief, the OptA sensor prototype used a QTF (100 kHz, Type TC-26, Conrad, Hirschau, Germany) as the sensing element. The sample flow was directed through one focal point of a custom-made aluminum ellipsoidal cavity, and the QTF was installed at the other focal point of the cavity, with the physical separation preventing deposition of BC in the sample flow on the QTF. In particular, the ultrasound generated after excitation of the BC particles by light pulses at the first focal point of the ellipsoid (FP1), placed within the sample flow, is transmitted within the ellipsoidal cavity and refocused onto the QTF at the second focal point (FP2) 50 mm away from its excitation (Figure 1a). In this design, the axis of the laser light used for the excitation of the ultrasound signals is placed perpendicular to the sample flow. The cavity is designed such that only constructive interference

occurs at FP2, allowing a strong acoustic signal to be detected at this point.

2.2. Experimental setup of the OptA sensor prototype during the shipboard campaign

We implemented the OptA sensor prototype on-board the Stena Germanica (IMO: 9145176, MMSI 266331000, operated by Stena Line), a RoPax ferry with four Wärtsilä four-stroke 8ZAL40S engines transporting passengers and cargo between Kiel, Germany and Gothenburg, Sweden. Figure 1b shows a schematic of the field test set-up. The field test of the OptA sensor prototype was conducted as part of the SCIPPER project campaign (Ntziachristos et al. 2023; Mamarikas et al. 2023), where multiple BC sensors were tested in parallel. Because most of the other sensors being tested during the campaign were filter-based systems, a dilution protocol was implemented for all sensors to allow the filter-based sensors to run continuously throughout the night without filter replacements. During the measurements, main engine 1 (ME1) was shut off and ME2 operated on high load.

The exhaust as it would be expelled to the atmosphere was fed through a dilution system (eDilutor, Dekati, Kangasala, Finland), which provided a diluted sample flow to the OptA sensor and all other sensors that were part of the Scipper campaign including the filter-based instrument (ObservAir, DSTech, Richmond, CA, USA) we used for comparison. The exhaust from main engine 2 (ME2) was transported from the diluter to the sensors *via* conductive tubes (Tygon by Saint-Gobain Ceramics and Plastics Inc., Solon, OH, USA) to avoid particle deposition in the sample lines due to charge build-up. The sensors were placed as close as

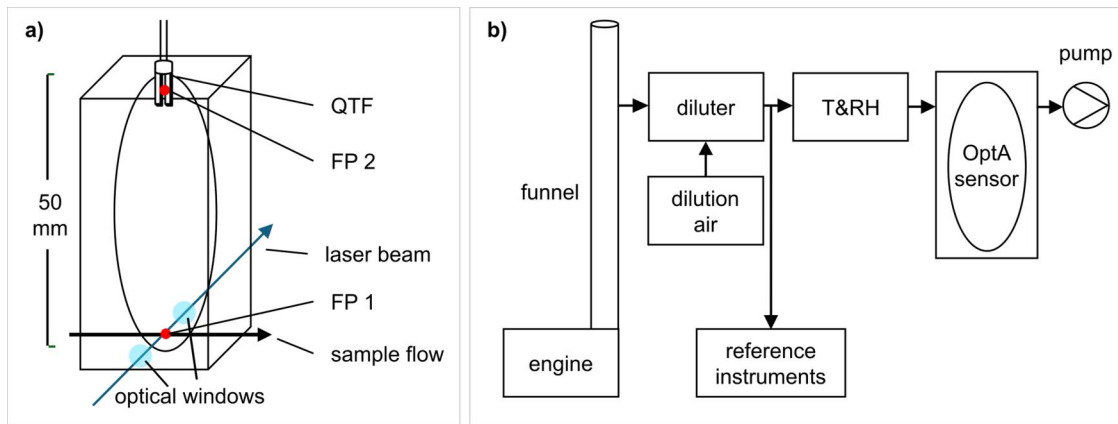


Figure 1. Schematic of the OptA sensor and its integration on-board the RoPax ferry. (a) Schematic of the OptA sensor depicting the ellipsoidal cavity. Laser excitation generates acoustic waves at focal point 1 (FP1) that are refocused at focal point 2 (FP2) where the quartz tuning fork (QTF) is placed. (b) Schematic of the sampling set-up for shipboard measurements. The arrows indicate the direction of sample flow. T&RH: temperature and humidity sensor; DAQ: data acquisition.

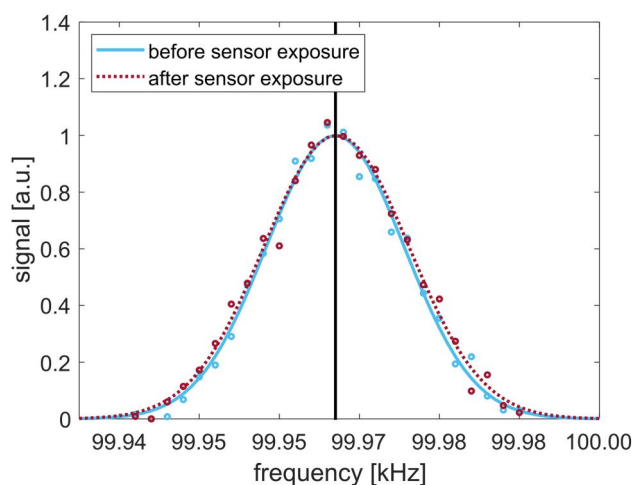


Figure 2. Quartz tuning fork (QTF) resonance curves before and after shipboard measurement. QTF resonance curves were generated from measurements acquired via a frequency sweep of the laser modulation. Signals (a.u.) were measured before and after measuring BC in ship exhaust. Gaussian fits were applied to the data. The resonant frequency is 99.967 kHz (black vertical line), which is the frequency that corresponds to the peak values of the Gaussian curve.

possible to the funnel and dilution system with approximately 1.5–2 m long sample lines with 6 mm diameter. With a flow of 2 lpm to the IDSS and a total flow of 7.42 lpm to a group of other sensors including the ObservAir, the particle residence times inside the tubes were 1.7 s and 0.5 s, respectively.

The IDSS and the ObservAir were used with a two-step dilution cycle, employing periodic flushing periods over a 9.5 h measurement, resulting in a net particle exposure time of approximately 2.6 h. The dilution protocol consisted of repeated cycles of three steps. First, sample flow was provided to the sensors for 2 min at a low dilution ratio ($DR = 1:75$). Second, sample flow was provided for 2 min at a high dilution ratio ($DR = 1:150$). The third cycle consisted of particle-free air and was set for 11 min. This dilution cycle was used for engine operation with marine gas oil (MGO). For engine operation with methanol the cycles were slightly different, i.e., a DR of 1:50 for 4 min, a DR of 1:150 for 4 min and a third cycle with particle-free air for 25 min.

During measurement, a temperature and humidity sensor (Si7021, Adafruit Industries, New York, NY, USA) controlled by an Arduino Uno (Arduino, Somerville, MA, USA) microcontroller board was placed between the dilutor and the OptA sensor prototype to monitor the temperature and humidity of the sample flow. Following this monitoring step, the sample flow was guided through FP1 of the cavity at a constant flowrate of 2 lpm, maintained by a pump at the sensor outlet. A laser beam was

propagated through FP1 perpendicular to the sample, with a focal point fixed at FP1. The beam was generated using a fiber-coupled butterfly laser diode with a wavelength of 450 nm (FBLD-450-0.800W-FC105-BTF, Frankfurt Laser Company, Frankfurt, Germany) and a commercial laser diode driver (BFS-VRM 03 HP, PicoLAS GmbH, Würselen, Germany). Fiber output was collimated using a fixed collimation package (F230SMA-A, Thorlabs, Newton, NJ, USA) and coupled to the sensor with a focusing lens (LA1560-A-ML, Thorlabs, Newton, NJ, USA). The laser was controlled by a function generator (33500b Trueform, Keysight, Santa Rosa, CA, USA) and modulated with a square wave whose frequency was tuned to the resonance frequency of the QTF (~ 100 kHz). The duty cycle of the modulation was 20%. A photodiode (DET10A2, Thorlabs, Newton, NJ, USA) monitored the laser output at the rear side of the sensor during all experiments.

During operation, the OptA signal was detected by the QTF, amplified by a custom-made amplifier circuit utilizing a dual operational amplifier (AD712D, Analog Devices, Norwood, MA, USA) and recorded using an 8-bit data acquisition card (Picoscope 3403D, Pico Technology Ltd., Cambridgeshire, UK). The signal was oversampled at 125 MS/s and then downsampled via averaging to 1 MS/s, effectively increasing the number of bits of the data acquisition. The acquisition time was 1 s with a 20 s pause between measurements to minimize laser heating.

For comparing the measured OptA signal of the IDSS to BC concentrations the ObservAir, an aerosol absorption photometer was available during the campaign. The instrument is filter-based and operates similar to aethalometers. It is typically used for ambient measurements (Hofman et al. 2024; Wu et al. 2024). The ObservAir was used during the campaign since it is relatively low in cost and small in size. Thus, it could be easily installed on-board in contrast to instruments such as the MSS. As the final aim of the IDSS's development is to create a low-cost and portable sensor the campaign was a good opportunity to compare the IDSS to a sensor with similar features (cost, size). The ObservAir received the BC sample from the eDilutor equivalently to the IDSS. The flow rate was set to 30 sccm (0.03 lpm). Since no fast changes in the BC concentrations in the ship's exhaust were expected a time base of 10 s was chosen, which gives a sufficient temporal resolution for long-term changes and constant BC concentration levels. After the 10 h operation period the instrument indicated a necessary filter change. Both IDSS and ObservAir

measure signals related to how light interacts with BC particles. However, the measurement principle itself is different. The IDSS measures an OptA signal which is directly proportional to the light absorption. The ObservAir measures the attenuation of light by BC particles that are collected on the filter. In the absence of light scattering agents, light absorption is the main factor contributing to the light attenuation. Thus, there is a good correlation between OptAS (PAS) and filter-based methods (Aakko-Saksa et al. 2021) with median values within 25% of each other as reported under laboratory conditions (Salo et al. 2024). Therefore, the ObservAir, which is based on an established method for BC measurements, was used for comparison but not as a reference to the IDSS.

2.3. Obtaining the resonance frequency of the QTF

To obtain the resonance frequency of the OptA sensor prototype's QTF, we performed a frequency sweep across a range of frequencies used during laser excitation. The frequency sweep was performed before and after the OptA sensor prototype's field test on-board the Stena Germanica. The noise floor was subtracted from the data sets and the data were normalized to the maximum value of each set of measurement. Gaussian fits were then applied to the data using Equation (1), where f refers to the intensity at frequency x . a , b , and c are coefficients defining the Gaussian. The amplitude a was normalized to one.

$$f(x) = a \cdot \exp\left(-\left(\frac{x-b}{c}\right)^2\right) \quad (1)$$

2.1. OptA signal conversion to BC concentration

We performed a zeroing-procedure of the raw data removing a signal offset calculated during flushing periods. Then, the OptA signal (x in μV) was converted to BC mass concentration (y in $\mu\text{g}/\text{m}^3$) using the linear fit of Figure 3 giving Equation (2).

$$y = 0.51 \cdot x \quad (2)$$

The first two dilution cycles were not considered in the fit due to unstable humidity levels. Furthermore, the last dilution cycle was not considered due to rapid changes in BC concentration. The fast dynamic leads to incorrect temporal alignment caused by unequal flows and time bases. Thus, the measurements of the two sensors are expected to exhibit larger deviations during the last cycle. For determining the engines exhaust before dilution, the measured BC concentration was multiplied by the corresponding dilution factor. The average and standard deviation of the resulting values are presented in Figure 4.

2.2. Calculating BC emission factors

To calculate the BC emission factor EF in $\text{g BC}/\text{kg fuel}$ for our measurements we use the tracer method

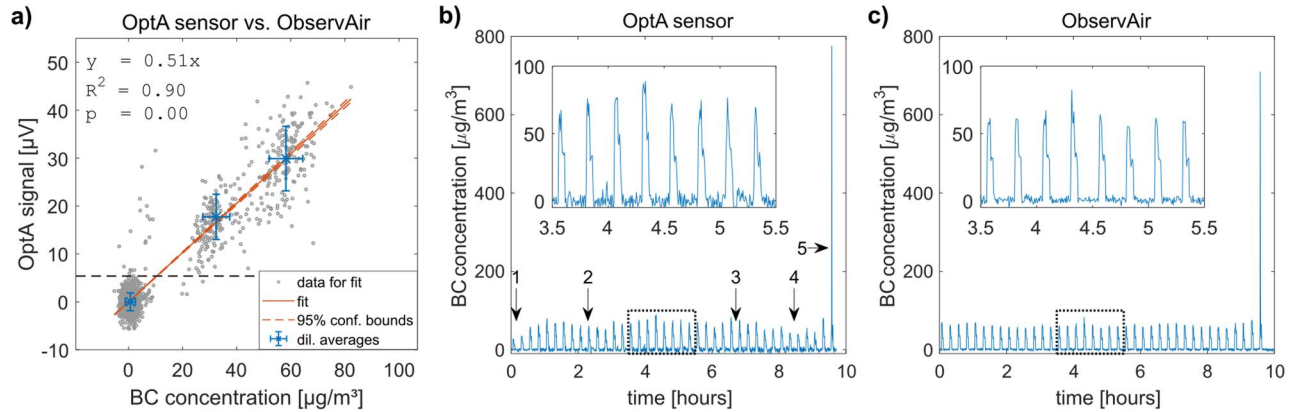


Figure 3. The optoacoustic (OptA) signal during shipboard measurements and comparison to the ObservAir's BC mass concentration. (a) Correlation plot for the OptA sensor and the ObservAir aerosol absorption photometer during the shipboard measurements. The raw signal of the OptA sensor is plotted in μV , while the response of the ObservAir is presented in $\mu\text{g}/\text{m}^3$. The data points used for the fit are plotted in grey, average values for each dilution cycle together with the standard deviation as error bars are plotted in blue. (b,c) Graphs show the data collected on-board the Stena Germanica by (b) the OptA sensor after background subtraction and conversion and (c) the ObservAir. The data shows the two-step dilution cycle and the flushing periods. Points labeled 1, 2, 3, and 4 refer to time points where the data from the OptA sensor deviate from the ObservAir. The large concentration peak (5) was captured during maneuvering in the harbor before engine shutdown.

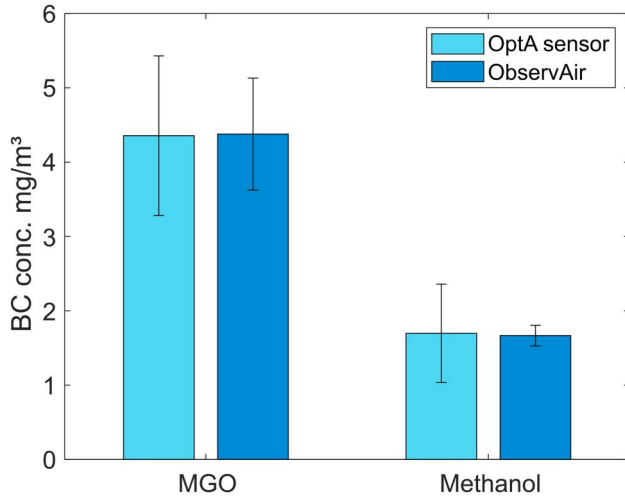


Figure 4. Black carbon (BC) concentrations of main engine 2 (ME2) running on marine gas oil (MGO) and methanol. The concentration of the ships exhaust for two different fuels measured by the OptA sensor (light blue) in comparison to the ObservAir (dark blue).

(Rönkkö et al. 2023) based on simultaneous CO_2 measurements. Following this method, the background concentration of BC is subtracted from the sample BC concentration and the resulted value is divided by the sample CO_2 concentration subtracted by the background CO_2 . The result is multiplied with the fuel's carbon mass fraction ($\text{kg CO}_2/\text{kg fuel}$). The following formula is used:

$$EF = \frac{BC_s \cdot DR - BC_d}{\rho_{\text{CO}_2}(\text{CO}_{2,s} - \text{CO}_{2,d})/100} \cdot EF_{\text{CO}_2} \quad (3)$$

In Equation (3) BC_s is the measured BC particles concentration in the diluted sample in g/m^3 , DR is the dilution ratio of the sample (dimensionless) and BC_d is the BC particles concentration in the dilution air in g/m^3 , which we assume is equal to zero. At the denominator, $\text{CO}_{2,s}$ is the raw CO_2 concentration of the sample which was measured during the campaign (Weisheit et al. 2022) and was 5.7% on average and $\text{CO}_{2,d}$ is the CO_2 concentration of the dilution air which is equal to 0.05%. Also, ρ_{CO_2} is the density of CO_2 in the sample, which is required to convert the measured CO_2 concentration from percentage to units of mass per volume (g/m^3). A density equal to 1.74 kg/m^3 is used assuming a sample temperature of 35°C and pressure of 1 bar.

Finally, EF_{CO_2} is the CO_2 emission factor of the fuel, which was calculated based on the fuel's elemental analysis (Weisheit et al. 2022). The fuel comprised of Carbon (C) by 86.5%, Hydrogen (H) by 12.3% and Oxygen (O) by 1.1%, with the rest 0.1% comprised by other substances (such as Sulfur and Nitrogen). EF_{CO_2} is calculated based on the following equation:

$$EF_{\text{CO}_2} = \frac{MB_{\text{CO}_2}}{MB_C} \text{Fuel}_C \quad (4)$$

where MB_{CO_2} is the molecular mass of CO_2 , which is equal to 44 g/mol , MB_C is the molecular mass of carbon (C), which is equal to 12 g/mol , and Fuel_C is the mass fraction of carbon in the fuel, which as mentioned before was measured at 86.5%. The result is that EF_{CO_2} is equal to 3.17.

3. Results

The IDSS was tested on-board the Stena Germanica, a RoPax ferry. The sensor measured the ship's exhaust after a dilution stage. First, the resonance curve of the transducer (a QTF) before and after the BC measurements, then the longitudinal measurements of the BC concentrations in comparison to the ObservAir will be presented. Finally, we will compare BC concentrations measured for two different fuel types (MGO and Methanol).

Figure 2 shows the resonance curves of the QTF obtained via a frequency sweep of the laser intensity modulation before and after the total BC measurement time, i.e., the time the OptA sensor was exposed to the BC sample, respectively. After sensor exposure, the resonance curve (Figure 2, dotted line) only minimally changed in comparison to the resonance curve before sensor exposure (Figure 2, solid line). In fact, the difference between the resonant frequencies of the curves was only 0.1 Hz, which lies well within the 95% confidence interval of $\pm 4 \text{ Hz}$.

The data of the OptA sensor of the entire 9.5 h measurement is plotted versus the BC concentration of the ObservAir (Figure 3a). Three regions can be distinguished, roughly at 0, 30 and $60 \mu\text{g/m}^3$ that correspond to the clean-air period and the high and low dilution ratios of the dilution cycle, respectively. Average values (blue) for each point in the dilution cycle are very close to the linear fit (red line), which was determined from the whole data set (grey). The noise equivalent concentration (NEC) (intersection of the fit with the dashed black line, Figure 3a) is $10.5 \mu\text{g/m}^3$ for 1 s integration time.

Figure 3b shows the data of the OptA sensor converted to BC concentration via the linear fit of Figure 3a over the entire measurement period of 9.5 h. For comparison, the BC concentration measured by the ObservAir is plotted in Figure 3b. Figures 3b and c demonstrate that the two sensors were able to quantify BC concentrations at two dilution ratios (DRs; 1:75 and 1:150) and during the flushing periods, resulting in similar plots reflecting the two-step

dilution cycle with intermediate flushing periods. Specifically, [Figures 3b and c](#) showed that the high DR halved (0.55 ± 0.077 for the OptA sensor prototype and 0.51 ± 0.075 for the ObservAir) the BC concentration compared to the low DR. The ratio was first calculated for each cycle individually. The means and standard deviations of these ratios are reported. Importantly, these calculated values are very close to the expected value of 0.5, which falls within their standard deviations.

Slight deviations can be observed in the data collected by the two sensors ([Figure 3](#)). [Figure 3b](#) shows that the OptA sensor prototype underestimates the BC concentration at the beginning of the measurement (arrow 1) due to humidity (see [the online supplementary information](#)). After the first few dilution cycles, a similar trend was observed for both sensors, albeit with slight differences. The OptA sensor prototype ([Figure 3b](#)) measured lower (arrows 2 and 4) or higher (arrow 3) BC concentrations than the ObservAir ([Figure 3c](#)), which had more stable readings over the measurement period. Both sensors detected a high particle concentration in the last cycle (arrow 5) with a BC concentration of $775 \mu\text{g}/\text{m}^3$ measured by the OptA sensor and $709 \mu\text{g}/\text{m}^3$ measured by the ObservAir with a duration <30 s. The actual spike duration could not be resolved as it was shorter than the 10 s averaging period of the ObservAir. This spike was due to the engines operating at a lower load factor while berthing in the harbor before the shutdown of the ship's engines. This means an increase of BC concentrations by a factor of ~ 13 can be observed inside the harbor during maneuvering in comparison to stable operation at sea. Considering the dilution ratios the concentration in-stack before the dilution system can be calculated. During stable operation, the mean concentration in the ship's exhaust was calculated to be $4.36 \text{ mg}/\text{m}^3$ for the OptA sensor and $4.38 \text{ mg}/\text{m}^3$ for the ObservAir.

The RoPax ferry's engines are modified such that methanol can be used as well. During a different day the OptA sensor was implemented to measure the exhaust of ME2 running on methanol. For both fuel types, the engine was running in similar operation conditions. The mean BC concentration in the funnel (before dilution) calculated from the measurements of the OptA sensor and the ObservAir for both fuel types is plotted in [Figure 4](#). The mean BC concentration for methanol is reduced significantly for both sensors. For the OptA sensor we have calculated a mean concentration of $1.70 \text{ mg}/\text{m}^3$ and for the ObservAir a mean concentration of $1.67 \text{ mg}/\text{m}^3$. We

therefore observe a reduction in BC concentration by 61% for the OptA sensor and by 62% for the ObservAir when the engine is operating on methanol instead of MGO.

4. Discussion

Demonstration of new technologies in real-world applications outside of laboratory environments is crucial for developing technology suitable for the challenging conditions of shipboard BC monitoring. For this reason, we demonstrated herein the application of the IDSS on-board a ship and found accurate determination of BC concentration changes in comparison to a commercial filter-based instrument. This sensor could address a gap in BC ship emission monitoring and enable the enforcement of regulations on ship emissions.

The delicate detector of the OptA sensor requires protection from contamination to maintain reliable operation over long periods of time. We showed that the QTF exhibited very similar resonance behavior before and after the longitudinal measurements presented in this paper. This finding implies that the spatial separation of illumination and detection achieved by the IDSS indeed protects the QTF from BC contamination. The separation of the QTF from the sample flow represents a marked improvement from previous QEPAS designs, in which the sensitive elements such as the QTF or additional resonators are directly in contact with the BC sample. In almost all cases, QEPAS sensors are used only to detect specific types of gases ([Patimisco et al. 2018](#)). In contrast, for measurements of exhaust, QEPAS gas sensors use filters to remove BC particles from the gaseous sample to avoid interference from soot ([Shi et al. 2017](#); [Breitenger et al. 2020](#)). To our knowledge, only one study has attempted to monitor BC with a conventional QEPAS setup in a laboratory environment. However, the study did not examine the effect of particle deposition on the QTF ([Breitenger et al. 2019](#)). The demonstrated IDSS performance is the first study showcasing QTF-based monitoring of BC particles in real environments. As a next step, we will investigate the performance of the IDSS under long-term exposure to establish the time frame of a recommended maintenance cycle.

On-board the RoPax ferry, the OptA sensor was able to accurately measure changes in BC concentration. We want to note that we did not experience any unusual behavior of the sensor on-board the ship different from observations in a laboratory environment

such as interference from other instruments or vibrational interferences. We gained insights in the exhaust under different operating conditions of the vessel, such as an increase of BC concentration during maneuvering or a decrease in BC concentration when using methanol instead of the conventional MGO. To establish control measures for vessel BC emission, such measurements provide valuable information and call for widespread implementation of BC sensors on-board of vessels. While there is a strong linear correlation between the IDSS and the ObservAir, data points deviating from the linear fit can be observed. The two instruments were not perfectly synchronized in BC sampling (different flow rates, sample lines and volumes) as well as in data acquisition. A higher standard deviation for the novel IDSS is expected as its time bases were shorter than the ObservAir's by one order of magnitude (1s vs. 10 s). Furthermore, temperature and humidity have an influence on both instruments. Filter-based instruments are known to be impacted by changes in the sample conditions such as temperature, humidity, pressure changes in the sampling lines, etc. (Backman et al. 2017, Ferrero et al. 2024). Since the acoustic wave propagates through air inside the ellipsoidal cavity, the OptA signal is also influenced by outside parameters such as temperature and humidity (Harris 1966). As we have seen this influence of humidity on the OptA signal (Figure 3 case 1), stable sampling conditions need to be ensured. If not, the sensor has to be characterized for different humidity levels and temperatures such that the signal can be compensated for. A cause of the fluctuations in Figure 3 case 4 could not be identified yet. Differences in results from different types of sensors have been linked to different particle properties (Momenimovahed et al. 2022). However, the load of the engine remained constant until maneuvering in the harbor. Thus, further investigation is required.

Currently, there is no standardized calibration protocol for BC instruments. In order to be able to compare the IDSS to the BC concentrations measured by the ObservAir, we converted the measured OptA signal via a linear correlation fit between the two instruments. However, we do not view this as a calibration method. Deviations are generally common for different BC instruments especially when they use different operating principles. Thus, it is necessary to establish a calibration protocol for the novel IDSS. Approaches such as creating absorbing aerosols from materials such as Aquadag or Nigrosin offer suitable options (Foster et al. 2019). Another method would be to calibrate the sensor gravimetrically by collecting

and weighing the BC particles originating from controlled BC generators (Schindler et al. 2004). However, such calibration protocols require additional facilities, which currently are not easily accessible. A standardized calibration method for BC monitoring needs to be established for widespread use.

During the campaign, we have observed a slight improvement of the NEC from $15.7 \mu\text{g}/\text{m}^3$ (Stylogiannis et al. 2021) to $10.5 \mu\text{g}/\text{m}^3$ for an integration time of 1 s, as expected since the laser power of the excitation was increased. However, such low detection limits are not necessary for shipboard monitoring. The high dilution ratios during the campaign were chosen to avoid frequent filter replacements of the ObservAir. Still the ObservAir indicated a necessary filter change after the measurement period. While we believe we can improve the sensitivity of the IDSS further, for applications with high contamination potential it is more important to concentrate on low-maintenance monitoring, which will be the focus to demonstrate for the IDSS.

The BC emissions of the Stena Germanica is close to the industry average meaning that our sensor should be able to monitor the majority of ships. Typical BC emission factors in the shipping industry range from 0.05 to 1.2 g BC/kg fuel, with the average for most ship categories being between ~ 0.4 and 0.6 g BC/kg fuel (Rönkkö et al. 2023). For the Stena Germanica, we estimated an emission factor of 0.15 g BC/kg fuel, assuming that the ship's exhaust contains 5.7% CO_2 , and that the ship has a CO_2 emission rate of 3.17 kg per kg of fuel with an accompanying BC concentration of $\sim 30 \mu\text{g}/\text{m}^3$ measured using a DR of 1:150. The average CO_2 concentration is based on exhaust measurements, while the emitted CO_2 per kg of fuel is based on an elemental analysis of the fuel (Weisheit et al. 2022). Larger emissions can be expected when the ship operates not only on one but two main engines in partial load operation (Weisheit et al. 2022). However, we have seen that the BC concentration reduces significantly when the RoPax ferry operates on methanol. Thus, a wide range of BC concentrations can be expected and dilution systems might need to be adjusted accordingly. Further work needs to be done to validate sensor performance using experimental models or tests on-board different ships in order to define a standard operating procedure suitable for monitoring BC emissions of ships for regulatory bodies.

Regarding the operational requirements of a monitoring system we have observed that the ship traveled at constant speed resulting in constant BC concentrations without rapid changes. The time bases of the sensors

were 10 s for the ObservAir and 1 s for the IDSS with a 21 s break between measurements, which is fast enough to capture the two steps of the dilution cycle (2 min each). However, fast temporal changes in the sample concentration were observed during maneuvering with a spike duration of <30 s. Meaning: faster acquisition protocols should be used during maneuvering, which can be implemented for the IDSS with smaller to no breaks between measurements resulting in a temporal resolution down to 1 s. Also, the ObservAir can provide a minimum temporal resolution of 2 s. We aim to employ a reference and sampling protocol that allows better time resolution in the future to capture the full dynamic of the emitted BC concentrations.

Potentially, more spikes in the BC concentration were missed by both sensors due to the 10 min particle-free dilution periods of the dilution cycle. Thus, uninterrupted sampling protocols without particle-free periods are recommended to capture the fast dynamic during ship maneuvering. This would increase the exposure to BC particles and most likely increase maintenance requirements of BC sensors. As a next step, we aim to test the IDSS with a continuous sampling protocol to capture the full dynamics of the BC sample and to fully investigate the need of cleaning maintenance under continuous and extended exposure.

To add to the potential of the IDSS, it is possible to extend its capabilities for more detailed BC characterization. For example, multi-wavelength excitation is possible by sequentially exciting the sample with a different wavelength by combining the output from different lasers and coupling into the IDSS. This would make the sensor suitable to measure optical properties of BC, such as the Ångström exponent (Moosmüller, Chakrabarty, and Arnott 2009). Together with additional methods, which determine the absolute mass of the sample (Petzold et al. 2013), the absorption coefficient can also be determined with the help of the IDSS.

With this first campaign, we have demonstrated the potential of the IDSS for real-life applications. As a next step, the sensor will be tested for long-term operation investigating sensor stability and ideally realizing low-maintenance monitoring. For example, the ObservAir requires a filter change after the measurement period presented in this paper, resulting in daily maintenance. Ideally, we will be able to present an OptA sensor prototype with much longer maintenance cycles resulting in low maintenance costs. Future designs could also incorporate inexpensive illumination from a new generation of high-intensity laser diodes (Stylogiannis et al. 2018, 2022), further reducing the overall cost. Together

with the inexpensive QTF, the cost of the IDSS will be significantly lower than currently available OptA instruments, such as the MSS (10–100 times lower). We estimate that the cost of the first version of the novel sensor will be similar to portable aethalometers or aerosol absorption photometers (e.g., microAeth, AethLabs or the ObservAir, DSTech), which in general are more affordable than currently available OptA instruments. However, omitting frequent maintenance will make the IDSS more cost efficient in comparison. The sensor presented in this work is still under development and the exact specifications will be established during a commercialization process. Nevertheless, the current demonstration points to IDSS as a potent technology for continuous operation, as appropriate for on-board emission monitoring in real-time. Due to the small size and cost, such design could also in the future be employed more broadly in environmental applications, i.e., large-scale spatial sampling within city, port or industrial grids for implementing real-time monitoring and smart city abilities.

Nomenclature

BC	black carbon
DR	dilution ratio
FP	focal point
FSN	filter smoke number
IDSS	illumination-detection separating sensor
IMO	International Maritime Organization
LII	laser induced incandescence
ME	main engine
MGO	marine gas oil
MSS	micro soot sensor
NEC	noise equivalent concentration
OptA	optoacoustic
OptAS	optoacoustic spectroscopy
PAS	photoacoustic spectroscopy
PAX	photoacoustic extinctions
PM	particulate matter
QEPAS	quartz enhanced photoacoustic spectroscopy
QTF	quartz tuning fork
RoPax	roll-on/roll-off ferry with passengers
RoRo	roll-on/roll-off ferry
SM	smoke meter
SOx	sulfur oxides

Acknowledgments

We thank Stena Line and the crew of the Stena Germanica for their collaboration and for welcoming us on-board. We thank everyone participating in the Scipper Campaign especially Jana Moldanova (IVL) for organizing, as well as the members from Tampere University Aerosol Physics Laboratory for providing the dilution system as well as the ObservAir setup and FMI for providing the ObservAir itself.


Disclosure statement

V.N. is a founder and equity owner of Maurus OY, sThesis GmbH, iThera Medical GmbH, Spear UG and I3 Inc. No potential conflict of interest was reported by the author(s).

Funding

This work was supported by the European Union's Horizon 2020 research and innovation programme under grant agreement No 814893 (SCIPPER) and under grant agreement No 862811 (RSENSE).

ORCID

Linda Haedrich  <http://orcid.org/0009-0001-2170-3034>
 Leonidas Ntziachristos  <http://orcid.org/0000-0002-5630-9686>
 Vasilis Ntziachristos  <http://orcid.org/0000-0002-9988-0233>

References

- Aakko-Saksa, P., N. Kuittinen, T. Murtonen, P. Koponen, M. Aurela, A. Järvinen, K. Teinilä, S. Saarikoski, L. M. F. Barreira, L. Salo, et al. 2021. Suitability of Different Methods for Measuring Black Carbon Emissions from Marine Engines. *Atmosphere* 13 (1):31. doi: [10.3390/atmos13010031](https://doi.org/10.3390/atmos13010031).
- Backman, J., L. Schmeisser, A. Virkkula, J. A. Ogren, E. Asmi, S. Starkweather, S. Sharma, K. Eleftheriadis, T. Uttal, A. Jefferson, et al. 2017. On Aethalometer measurement uncertainties and an instrument correction factor for the Arctic. *Atmos. Meas. Tech.* 10 (12):5039–62. doi: [10.5194/amt-10-5039-2017](https://doi.org/10.5194/amt-10-5039-2017).
- Bond, T. C., S. J. Doherty, D. W. Fahey, P. M. Forster, T. Bernsten, B. J. DeAngelo, M. G. Flanner, S. Ghan, B. Kärcher, D. Koch, et al. 2013. Bounding the role of black carbon in the climate system: A scientific assessment. *JGR. Atmospheres*. 118 (11):5380–552. doi: [10.1002/jgrd.50171](https://doi.org/10.1002/jgrd.50171).
- Breitegger, P., M. A. Schriebl, R. T. Nishida, S. Hochgreb, and A. Bergmann. 2019. Soot mass concentration sensor using quartz-enhanced photoacoustic spectroscopy. *Aerosol Sci. Technol.* 53 (9):971–5. doi: [10.1080/02786826.2019.1635677](https://doi.org/10.1080/02786826.2019.1635677).
- Breitegger, P., B. Schweighofer, H. Wegleiter, M. Knoll, B. Lang, and A. Bergmann. 2020. Towards low-cost QEPAS sensors for nitrogen dioxide detection. *Photoacoustics* 18: 100169. doi: [10.1016/j.pacs.2020.100169](https://doi.org/10.1016/j.pacs.2020.100169).
- Capderou, M. 2014. Geometry of the Ellipse. In *Handbook of satellite orbits: From Kepler to GPS*, 1–23. Cham: Springer. doi: [10.1007/978-3-319-03416-4_1](https://doi.org/10.1007/978-3-319-03416-4_1).
- Coen, M. C., E. Weingartner, A. Apituley, D. Ceburnis, R. Fierz-Schmidhauser, H. Flentje, J. S. Henzing, S. G. Jennings, M. Moerman, A. Petzold, et al. 2010. Minimizing light absorption measurement artifacts of the Aethalometer: Evaluation of five correction algorithms. *Atmos. Meas. Tech.* 3 (2):457–74. doi: [10.5194/amt-3-457-2010](https://doi.org/10.5194/amt-3-457-2010).
- Davies, N. W., C. Fox, K. Szpek, M. I. Cotterell, J. W. Taylor, J. D. Allan, P. I. Williams, J. Trembath, J. M. Haywood, and J. M. Langridge. 2019. Evaluating biases in filter-based aerosol absorption measurements using photoacoustic spectroscopy. *Atmos. Meas. Tech.* 12 (6):3417–34. doi: [10.5194/amt-12-3417-2019](https://doi.org/10.5194/amt-12-3417-2019).
- Drinovec, L., G. Močnik, P. Zotter, A. S. H. Prévôt, C. Ruckstuhl, E. Coz, M. Rupakheti, J. Sciare, T. Müller, A. Wiedensohler, et al. 2015. The "dual-spot" Aethalometer: An improved measurement of aerosol black carbon with real-time loading compensation. *Atmos. Meas. Tech.* 8 (5):1965–79. doi: [10.5194/amt-8-1965-2015](https://doi.org/10.5194/amt-8-1965-2015).
- Ferrero, L., N. Losi, M. Rigler, A. Gregorič, C. Colombi, L. D'Angelo, E. Cuccia, A. M. Cefalì, I. Gini, A. Doldi, et al. 2024. Determining the Aethalometer multiple scattering enhancement factor C from the filter loading parameter. *Sci. Total Environ.* 917:170221. doi: [10.1016/j.scitotenv.2024.170221](https://doi.org/10.1016/j.scitotenv.2024.170221).
- Foster, K., R. Pokhrel, M. Burkhart, and S. Murphy. 2019. A novel approach to calibrating a photo-acoustic absorption spectrometer using polydisperse absorbing aerosol. *Atmos. Meas. Tech.* 12 (6):3351–63. doi: [10.5194/amt-12-3351-2019](https://doi.org/10.5194/amt-12-3351-2019).
- Grahame, T. J., R. Klemm, and R. B. Schlesinger. 2014. Public health and components of particulate matter: The changing assessment of black carbon. *J. Air Waste Manag. Assoc.* 64 (6):620–60. doi: [10.1080/10962247.2014.912692](https://doi.org/10.1080/10962247.2014.912692).
- Harmesen, M. J. H. M., P. van Dorst, D. P. van Vuuren, M. van den Berg, R. Van Dingenen, and Z. Klimont. 2020. Co-benefits of black carbon mitigation for climate and air quality. *Clim. Change* 163 (3):1519–38. doi: [10.1007/s10584-020-02800-8](https://doi.org/10.1007/s10584-020-02800-8).
- Harris, C. M. 1966. Absorption of sound in air versus humidity and temperature. *J. Acoust. Soc. Am.* 40 (1): 148–59. doi: [10.1121/1.1910031](https://doi.org/10.1121/1.1910031).
- Hoesly, R., S. J. Smith, N. Prime, H. Ahsan, H. Suchyta, P. O'Rourke, M. Crippa, Z. Klimont, D. Guizzardi, J. Behrendt, et al. 2024. Community Emissions Data System (CEDS) v_2024_07_08 Release Emission Data (Version v_2024_07_08) [Data set]. Zenodo. doi: [10.5281/zenodo.12803197](https://doi.org/10.5281/zenodo.12803197).
- Hofman, J., B. Lazarov, C. Stroobants, E. Elst, I. Smets, and M. Van Poppel. 2024. Portable sensors for dynamic exposure assessments in urban environments: state of the science. *Sensors* 24 (17):5653. doi: [10.3390/s24175653](https://doi.org/10.3390/s24175653).
- International Maritime Organization (IMO). 2011. Marine Environment Protection Committee – 62nd session, Agenda Item 4 (MEPC 62/4/3), Prevention of air pollution from ships: Reduction of emissions of Black Carbon from shipping in the Arctic, 8 April 2011.
- International Maritime Organization (IMO). 2015. Marine Environment Protection Committee – 68th session, Agenda Item 21 (MEPC 68/21), Report of the Marine Environment Protection Committee on its sixty-eighth session, 29 May 2015.
- International Maritime Organization (IMO). 2018. Subcommittee on pollution prevention and response - 5th session, Agenda Item 24 (PPR/5/24), Report to the Marine Environment Protection Committee, 23 March 2018.
- Janssen, N. A. H., G. Hoek, M. Simic-Lawson, P. Fischer, L. van Bree, H. ten Brink, M. Keuken, R. W. Atkinson, H. R. Anderson, B. Brunekreef, et al. 2011. Black carbon as an additional indicator of the adverse health effects of airborne

- particles compared with PM₁₀ and PM_{2.5}. *Environ. Health Perspect.* 119 (12):1691–9. doi: [10.1289/ehp.1003369](https://doi.org/10.1289/ehp.1003369).
- Johnson, K., W. Miller, T. Durbin, Y. Jiang, J. Yang, G. Karavalakis, and D. Cocker. 2017. Black carbon measurement methods and emission factors from ships. Consultant Report prepared for: International Council on Clean Transportation, Washington, DC, USA. Report Prepared by: University of California, Riverside, December 2016.
- Kang, S. C., Y. L. Zhang, Y. Qian, and H. L. Wang. 2020. A review of black carbon in snow and ice and its impact on the cryosphere. *Earth. Sci. Rev.* 210:103346. doi: [10.1016/j.earscirev.2020.103346](https://doi.org/10.1016/j.earscirev.2020.103346).
- Kosterev, A. A., Y. A. Bakhirkin, R. F. Curl, and F. K. Tittel. 2002. Quartz-enhanced photoacoustic spectroscopy. *Opt. Lett.* 27 (21):1902–4. doi: [10.1364/Ol.27.001902](https://doi.org/10.1364/Ol.27.001902).
- Lappi, M. K., and J. M. Ristimäki. 2019. Comparison of filter smoke number and elemental carbon from thermal optical analysis of marine diesel engine exhaust. *Proc. Institut. Mech. Eng. Part M-J. Eng. Marit. Environ.* 233 (2):602–9. doi: [10.1177/1475090218776196](https://doi.org/10.1177/1475090218776196).
- Ma, Y. F. 2018. Review of recent advances in QEPAS-based trace gas sensing. *Applied Sciences* 8 (10):1822. doi: [10.3390/app8101822](https://doi.org/10.3390/app8101822).
- Mamarikas, S., V. Matthias, M. Karl, L. Fink, P. Simonen, J. Keskinen, M. D. Maso, E. Fridell, J. Moldanova, Å. Hallquist, et al. 2023. Assessing shipping induced emissions impact on air quality with various techniques: Initial results of the SCIPPER project. *Transp. Res. Procedia*. 72:2141–8. doi: [10.1016/j.trpro.2023.11.699](https://doi.org/10.1016/j.trpro.2023.11.699).
- Michelsen, H. A., C. Schulz, G. J. Smallwood, and S. Will. 2015. Laser-induced incandescence: Particulate diagnostics for combustion, atmospheric, and industrial applications. *Prog. Energy Combust. Sci.* 51:2–48. doi: [10.1016/j.pecs.2015.07.001](https://doi.org/10.1016/j.pecs.2015.07.001).
- Momenimovahed, A., S. Gagné, P. Martens, G. Jakobi, H. Czech, V. Wichmann, B. Buchholz, R. Zimmermann, B. Behrends, and K. A. Thomson. 2022. Comparison of black carbon measurement techniques for marine engine emissions using three marine fuel types. *Aerosol Sci. Technol.* 56 (1):46–62. doi: [10.1080/02786826.2021.1967281](https://doi.org/10.1080/02786826.2021.1967281).
- Moosmüller, H., R. K. Chakrabarty, and W. P. Arnott. 2009. Aerosol light absorption and its measurement: A review. *J. Quant. Spectrosc. Radiat. Transf.* 110 (11):844–78. doi: [10.1016/j.jqsrt.2009.02.035](https://doi.org/10.1016/j.jqsrt.2009.02.035).
- Ng, A. K. Y., J. Andrews, D. Babb, Y. F. Lin, and A. Becker. 2018. Implications of climate change for shipping: Opening the Arctic seas. *Wiley Interdisciplinary Reviews-Climate Change* 9 (2):e507. doi: [10.1002/wcc.507](https://doi.org/10.1002/wcc.507).
- Ntziachristos, L., N. Kousias, V. Ntziachristos, A. Kontses, and A. Stylogiannis. 2021. Optoacoustic fluid sensing apparatus. US Patent 18/251,275, filed October 29, 2021 and issued December 21, 2023.
- Ntziachristos, L., S. Mamarikas, R. Verbeek, and A. Grigoriadis. 2023. Monitoring shipping emissions with various techniques towards ensuring compliance to the new regulations: The SCIPPER project. Paper presented at the SNAME 8th International Symposium on Ship Operations, Management and Economics, Athens, Greece, March 2023. doi: [10.5957/SOME-2023-019](https://doi.org/10.5957/SOME-2023-019).
- Patimisco, P., G. Scamarcio, F. K. Tittel, and V. Spagnolo. 2014. Quartz-enhanced photoacoustic spectroscopy: A review. *Sensors* 14 (4):6165–206. doi: [10.3390/s140406165](https://doi.org/10.3390/s140406165).
- Patimisco, P., A. Sampaolo, L. Dong, F. Tittel, and V. Spagnolo. 2018. Recent advances in quartz enhanced photoacoustic sensing. *Appl. Phys. Rev.* 5 (1):011106. doi: [10.1063/1.5013612](https://doi.org/10.1063/1.5013612).
- Petzold, A., J. A. Ogren, M. Fiebig, P. Laj, S.-M. Li, U. Baltensperger, T. Holzer-Popp, S. Kinne, G. Pappalardo, N. Sugimoto, et al. 2013. Recommendations for reporting “black carbon” measurements. *Atmos. Chem. Phys.* 13 (16):8365–79. doi: [10.5194/acp-13-8365-2013](https://doi.org/10.5194/acp-13-8365-2013).
- Pörtner, H., D. Roberts, E. Poloczanska, K. Mintenbeck, M. Tignor, A. Alegria, M. Craig, S. Langsdorf, S. Löschke, and V. Möller. 2022. IPCC, 2022: Summary for policy-makers. In *Climate change 2022: Impacts, adaptation and vulnerability. Contribution of working Group II to the sixth assessment report of the intergovernmental panel on climate change*, 3–33. Cambridge, UK: Cambridge University Press. doi: [10.1017/9781009325844.001](https://doi.org/10.1017/9781009325844.001).
- Rönkkö, T., S. Saarikoski, N. Kuittinen, P. Karjalainen, H. Keskinen, A. Järvinen, F. Mylläri, P. Aakko-Saksa, and H. Timonen. 2023. Review of black carbon emission factors from different anthropogenic sources. *Environ. Res. Lett.* 18 (3):033004. doi: [10.1088/1748-9326/acbb1b](https://doi.org/10.1088/1748-9326/acbb1b).
- Salo, L., K. Saarnio, S. Saarikoski, K. Teinilä, L. M. F. Barreira, P. Marjanen, S. Martikainen, H. Keskinen, K. Mustonen, T. Lepistö, et al. 2024. Black carbon instrument responses to laboratory generated particles. *Atmos. Pollut. Res.* 15 (5):102088. doi: [10.1016/j.apr.2024.102088](https://doi.org/10.1016/j.apr.2024.102088).
- Shi, C., D. Wang, Z. Wang, L. Ma, Q. Wang, K. Xu, S. Chen, and W. Ren. 2017. A mid-infrared fiber-coupled QEPAS nitric oxide sensor for real-time engine exhaust monitoring. *IEEE Sensors J.* 17 (22):7418–24. doi: [10.1109/JSEN.2017.2758640](https://doi.org/10.1109/JSEN.2017.2758640).
- Schindler, W., C. Haisch, H. A. Beck, R. Niessner, E. Jacob, and D. Rothe. 2004. A photoacoustic sensor system for time resolved quantification of diesel soot emissions. *SAE Trans.* 113:483–90. doi: [10.4271/2004-01-0968](https://doi.org/10.4271/2004-01-0968).
- Sorte, S., V. Rodrigues, C. Borrego, and A. Monteiro. 2020. Impact of harbour activities on local air quality: A review. *Environ. Pollut.* 257:113542. doi: [10.1016/j.envpol.2019.113542](https://doi.org/10.1016/j.envpol.2019.113542).
- Stylogiannis, A., N. Kousias, A. Kontses, L. Ntziachristos, and V. Ntziachristos. 2021. A low-cost optoacoustic sensor for environmental monitoring. *Sensors* 21 (4):1379. doi: [10.3390/s21041379](https://doi.org/10.3390/s21041379).
- Stylogiannis, A., L. Prade, A. Buehler, J. Aguirre, G. Sergiadis, and V. Ntziachristos. 2018. Continuous wave laser diodes enable fast optoacoustic imaging. *Photoacoustics* 9:31–8. doi: [10.1016/j.pacs.2017.12.002](https://doi.org/10.1016/j.pacs.2017.12.002).
- Stylogiannis, A., L. Prade, S. Glasl, Q. Mustafa, C. Zakian, and V. Ntziachristos. 2022. Frequency wavelength multiplexed optoacoustic tomography. *Nat. Commun.* 13 (1):4448. doi: [10.1038/s41467-022-32175-6](https://doi.org/10.1038/s41467-022-32175-6).
- Timonen, H., P. Karjalainen, P. Aalto, S. Saarikoski, F. Mylläri, N. Karvosenoja, P. Jalava, E. Asmi, P. Aakko-Saksa, N. Saukkonen, et al. 2019. Adaptation of black carbon footprint concept would accelerate mitigation of global warming. *Environ. Sci. Technol.* 53 (21):12153–5. doi: [10.1021/acs.est.9b05586](https://doi.org/10.1021/acs.est.9b05586).

- Timonen, H., P. Aakko-Saksa, N. Kuittinen, P. Karjalainen, T. Murtonen, K. Lehtoranta, H. Vesala, M. Bloss, S. Saarikoski, and P. Koponen. 2017. *Black carbon measurement validation onboard (SEA-EFFECTS BC WP2)*. Espoo, Finland: VTT Technical Research Centre of Finland.
- Weisheit, J., R. Verbeek, P. P. V. Verhagen, M. Irjala, P. Simonen, N. Kousias, J. Moldanova, L. Merelli, T. Smyth, A. Deakin, et al. 2022. Deliverable D1.6: Conclusions of technical possibilities of onboard sensor monitoring. Shipping Contributions to Inland Pollution Push for the Enforcement of Regulations (SCIPPER) Project.
- Wu, L., Y. Shen, F. Che, Y. Zhang, J. Gao, and C. Wang. 2024. Evaluating the performance and influencing factors of three portable black carbon monitors for field measurement. *J. Environ. Sci.* 139:320–33. doi: [10.1016/j.jes.2023.05.044](https://doi.org/10.1016/j.jes.2023.05.044).